Comparative Study of Identity Proton-Transfer Reactions between Simple Atoms or Groups by VB Methods

Wei Wu,[†] Sason Shaik,[‡] and William H. Saunders, Jr.*[,§]

Department of Chemistry, The State Key Laboratory for Physical Chemistry of Solid Surfaces and Institute of Physical Chemistry, Xiamen University, Xiamen 361005, People's Republic of China, Department of Organic Chemistry and the Lise Meitner-Minerva Center for Computational Quantum Chemistry, The Hebrew University, Jerusalem, 91904 Israel, and Department of Chemistry, University of Rochester, River Station, Rochester, New York 14627-0216

Received: June 19, 2002; In Final Form: September 30, 2002

Valence bond SCF calculations have been carried out on identity proton transfers of the type $X-H + X^- \rightarrow X^- + H-X$ and $X-H^+ + X \rightarrow X + X-H^+$ for systems where $X = F^-$, Cl^-, Br^-, OH^-, SH^-, NH_2^-, PH_2^-, CH_3^-, SiH_3^-, OH_2, NH_3, and PH_3. A hybrid consisting of three contributing structures—reactantlike, productlike, and ionic ($X^- H^+ X^-$ or $X H^+ X$)—gives reasonable results, though additional structures afford a slight further decrease in energy. Energies somewhat below Hartree−Fock and reasonable weights are obtained. Calculated barriers agree well with those obtained by high-level ab initio calculations with correlation. Insights into the factors determining barrier height are obtained.

I. Introduction

Proton transfers are either the main process or an essential part of the overall process in many chemical reactions. They have been extensively studied by ab inito methods, which have cast considerable light on the structures and electron distributions in the reactant complexes and transition structures of these reactions. It is not the purpose of this paper to review the extensive literature, but a particularly useful recent example is furnished by Gronert, who examined the potential energy surfaces for identity reactions of the first- and second-row nonmetal hydrides with their conjugate bases.[1] The calculations were carried out at the MP4/6-311+G(d,p)//MP2/6-31+G(d,p) and G2+ levels. DFT methods have been applied to identity reactions of a set of first-row hydrides.[2] We were interested in determining what insights might result from the application of valence bond self-consistent field (VBSCF) methods to a simple set of reactions similar to that of Gronert, particularly in view of our success in elucidating the factors responsible for nonperfect synchronization in proton transfers leading to resonance-stabilized conjugate bases.[3] The valence bond treatment of barriers to chemical reactions was outlined by one of us in 1981.[4]

II. Computational Methods

Preliminary structures were obtained using 6-31G basis sets in Gaussian 98.[5] The reactant was taken as the ion−dipole structure. The transition structure was taken as one in which the proton in transit was equally bonded to the donor and acceptor atoms. The donor and acceptor species involved were F^-, Cl^-, Br^-, OH^-, SH^-, NH_2^-, PH_2^-, CH_3^-, SiH_3^-, OH_2, NH_3, and PH_3. Where the species was a single atom, the Gaussian-optimized linear XHX structures were used unchanged. In the other cases, structures were modified so as to separate cleanly the active electrons from those that were frozen. For CH_3^-, SiH_3^-, NH_3, and PH_3, the attached protons were taken as linear combinations, $H_a + H_b + H_c$, which confine both the electrons directly involved in the proton transfer and the electrons involved in bonding to the attached hydrogens to the *z* axis, thus permitting the freezing of electrons in the p_x- and p_y-type orbitals and the exclusion of these orbitals from the active set, which then consisted only of s and p_z types. A similar tactic was used for NH_2^-, PH_2^-, and OH_2, but the groups attached to the heavy atom were planarized at the cost of a few kilocalories of energy so that the attached hydrogens could be taken as linear combinations, $H_a + H_b$, again enabling active electrons to be confined to the *z* axis. With OH^- and SH^-, a similar approach could not be used, for linearizing the H−X−H angles resulted in an unacceptable increase in energy. In these cases, both p_z- and p_x-type orbitals were included in the active set. The minimum possible number of electrons in the active set is four—the X−H bonding electrons plus the unshared pair on the acceptor atom. More realistic results were obtained using eight active electrons, with the additional four corresponding to unshared electrons on the monatomic donor and acceptor species and to unshared and/or X−H bonding electrons on the polyatomic species. In the case of OH^- and SH^-, better convergence and more realistic results were obtained with 12 active electrons, where the additional 4 correspond to those in the p_x-type orbitals. We next transformed the integrals from the Gaussian calculations to a valence bond basis set by utilizing the Xiamen programs.[6] Molecular orbitals with large coefficients for the active atomic orbitals were chosen as the active set: 2 for the minimum case, 4 in the cases reported in this article, and 6 for the 12-electron active sets (OH^- and SH^-). The remaining

* Corresponding author. E-mail: saunders@chem.chem.rochester.edu.
[†] Xiamen University.
[‡] The Hebrew University.
[§] University of Rochester.

10.1021/jp021452w CCC: $22.00
Published on Web 11/02/2002

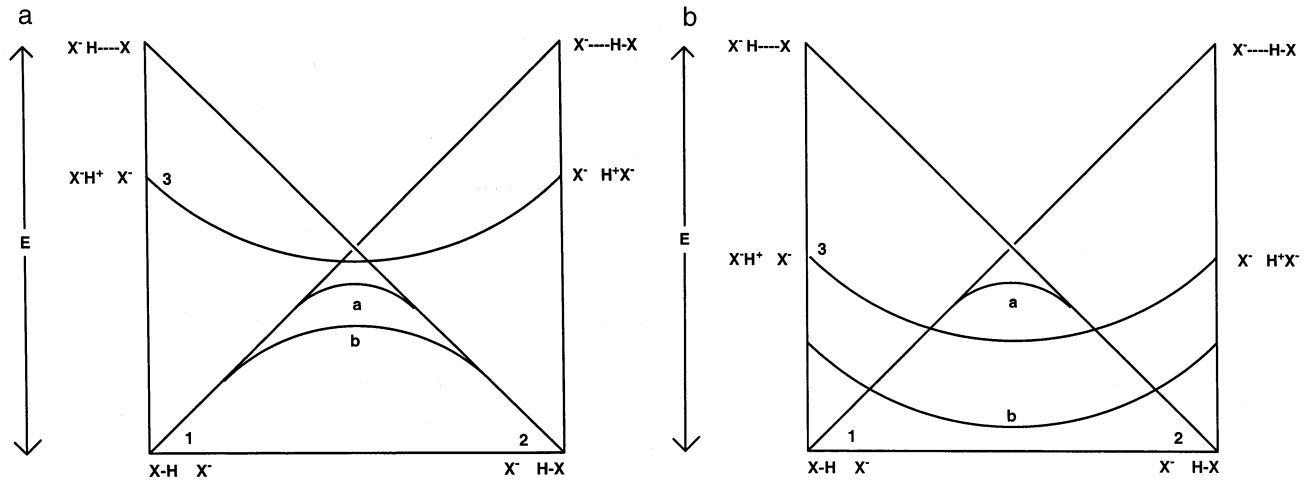

Figure 1. (a) Schematic diagram of the energies of contributing structures (**1**−**3**) and of the hybrids in the identity proton transfer $XH + X^- \rightarrow X^- + HX$ for the case where **3** is of high energy and hybrid **II** (curve b) is at a maximum. Curve a corresponds to the mixing of **1** and **2** (**1** ↔ **2**), and curve b, to the mixing of **1**−**3**. (b) Schematic diagram of the energies of contributing structures and of the hybrids in the identity proton transfer $XH + X^- \rightarrow X^- + HX$ for the case where **3** is of low energy and hybrid **II** (curve b) is at a minimum. Curve a corresponds to the mixing of **1** and **2** (**1** ↔ **2**), and curve b, to the mixing of **1**−**3**.

TABLE 1: Key to Contributing Structures[a]

number	designation	structure
1	L-1	$X-H\ X^-$
2	R-1	$X^-\ H-X$
3	I-1	$X^-\ H^+\ X^-$
4	I-2	$X^+\ H^-\ X^-$
5	I-3	$X^-\ H^-\ X^+$
6	LB	$X^\bullet\ H^-\ X^\bullet$

[a] 2-structure hybrid (**I**) uses **1** and **2**; 3-structure hybrid (**II**) uses **1**−**3**; 4-structure hybrid (**III**) uses **1**−**3** and **6**; and 6-structure hybrid (**IV**) uses **1**−**6**.

orbitals, including those corresponding to innershell electrons, were frozen.

III. Discussion

To carry out a VBSCF calculation, it is first necessary to choose a set of structures that contribute to the resonance hybrid. Our procedure was to start with the minimum number of structures possible, **1** and **2** (see Table 1 for descriptions of the contributing structures and hybrids). The position of the transition structure is then determined as shown in Figure 1a. Reactantlike structure **1** is of lowest energy when the X−H bond is of normal length. The energy rises as the bond is stretched to the length it possesses in the product. The reverse is true of productlike structure **2**. It is of high energy at the reactant X−H bond length and of low energy at the product. The location of transition structure **I** (**1** ↔ **2**) is then determined by the crossing point of these two curves, with the energy of the transition structure lower than that at the crossing point by the resonance energy from the interaction of the two structures (see upward-curved line a in Figure 1a).

These two structures are not adequate to give a proper description of the energy or electron distribution of the transition structure. At least one more contributing structure, "triple ion" **3**, is needed. The curve for the triple ion in Figure 1a is lowest at the crossing point and rises as the proton is moved toward one X or the other. The interaction of **3** with the hybrid of **1** and **2** to give **II** (**3** ↔ **I**) affords a further lowering of the energy to the upward-curved line b in Figure 1a and contributes needed ionic character to the transition structure. Further minor lowering of the energy and adjustment of the electron distribution is achieved by mixing in "reversed polarity" structures **4** and **5** and"long bond" structures **6**, so called because the single electrons on the two end atoms possess opposite spins and so can interact at a distance.

The exact energy and electronic structure of hybrid **IV** (**4**−**6** ↔ **II**) depend on the relative contributions of **1**−**6** to the overall hybrid. The ionic character of the complex and the transition structure is particularly strongly affected by the contribution of **3**. When **3** is relatively high in energy, it will not contribute much to the hybrid, and the X−H bonds at the transition state will be largely covalent. As the energy of **3** decreases relative to that of **1** and **2**, the transition-state bonds will have dominant ionic character, and the energy of the transition state will be lower. In the extreme case of **3** being much lower in energy than **1** and **2**, the X−H bonds will become mainly ionic, and the transition structure will disappear and be replaced by a symmetric complex located at an energy minimum as shown by downward-curved line b in Figure 1b. This is the case for two of the systems studied, $(H_2O\text{- - -H- - -}OH_2)^+$ and $(F\text{- - -H- - -}F)^-$, which are already stable symmetric species at the Hartree−Fock level.

Our calculations initially utilized the minimum number of active electrons, four, and two methods, the simple VB and the breathing orbital VB (BOVB).[7] In the simple VB method, the electron distribution in the fragments is taken to be the same regardless of whether the fragment is part of a two-electron bond or is ionic. Thus, X in X−H and in X^- are treated the same. In the BOVB method, X and H fragments in different bonding situations are allowed to optimize independently, giving, for example, different electron distributions for X in X−H and X^-. The results of these initial calculations are given in the Supporting Information. The results in Tables 2−6 are for 8-electron simple VB calculations, with 12-electron calculations also listed for the HOHOH and HSHSH systems (vide supra). These were chosen for detailed presentation because the 4-electron VB and BOVB calculations were found to exaggerate the ionic character of the X−H bonding in the transition structures and especially in the ion−dipole complexes.

Let us consider first the energies of the transition structures (Table 2) and the reactants and products (Table 4). The individual contributors, especially **1** and **2**, have energies well above the Hartree−Fock values from the SCFMO calculations. Only the hybrids of three or more structures have energies below

TABLE 2: Energies of Resonance Contributors and Hybrids for Transition Structures X−H−X[a]

X	*E*(HF/6-31G)	structures	*E*(str)	*E*(rel)	structures	*E*(str)	*E*(rel)
CH_3	−79.623872	L-1	−79.456363	105.1	3	−79.629991	−3.8
		R-1	−79.456363	105.1	4	−79.631157	−4.6
		I-1	−79.514361	68.7	6	−79.632218	−5.2
		2	−79.593477	19.1			
NH_2	−111.639129	L-1	−111.391004	155.7	3	−111.642512	−2.1
		R-1	−111.391004	155.7	4	−111.643107	−2.5
		I-1	−111.543821	59.8	6	−111.644499	−3.4
		2	−111.567211	45.1			
PH_2	−684.148335	L-1	−684.031957	73.0	3	−684.166503	−11.4
		R-1	−684.031957	73.0	4	−684.168984	−13.0
		I-1	−684.015385	83.4	6	−684.168984	−13.0
		2	−684.147083	0.8			
OH	−151.356029	L-1	−151.125632	144.6	3	−151.356582	−0.3
		R-1	−151.125632	144.6	4	−151.359595	−2.2
		I-1	−151.348874	4.5	6	−151.362950	−4.3
		2	−151.226214	81.5			
OH[b]	−151.356029	L-1	−151.110269	154.2	3	−151.358514	−1.6
		R-1	−151.110269	154.2	4	−151.360302	−2.7
		I-1	−151.250207	66.4	6	−151.362301	−3.9
		2	−151.242500	71.2			
SH	−796.722675	L-1	−796.556691	104.2	3	−796.722661	0.0
		R-1	−796.556691	104.2	4	−796.725275	−1.6
		I-1	−796.721224	0.9	6	−796.732047	−5.9
		2	−796.680148	26.7			
SH[b]	−796.722675	L-1	−796.600951	76.4	3	−796.725767	−1.9
		R-1	−796.600951	76.4	4	−796.729019	−4.0
		I-1	−796.569349	96.2	6	−796.729061	−4.0
		2	−796.698261	15.3			
F	−199.429704	L-1	−199.039327	245.0	3	−199.435561	−3.7
		R-1	−199.039327	245.0	4	−199.438069	−5.2
		I-1	−199.320534	68.5	6	−199.440527	−6.8
		2	−199.261589	105.5			
Cl	−919.600678	L-1	−919.440716	100.4	3	−919.604118	−2.2
		R-1	−919.440716	100.4	4	−919.607188	−4.1
		I-1	−919.452071	93.3	6	−919.607294	−4.2
		2	−919.555757	28.2			
Br	−5140.190466	L-1	−5140.034596	97.8	3	−5140.185287	3.2
		R-1	−5140.034596	97.8	4	−5140.189107	0.9
		I-1	−5140.016494	109.2	6	−5140.189108	0.9
		2	−5140.155682	21.8			
NH_3	−112.724233	L-1	−112.458200	166.9	3	−112.729560	−3.3
		R-1	−112.458200	166.9	4	−112.730354	−3.8
		I-1	−112.620093	65.3	6	−112.731665	−4.7
		2	−112.644362	50.1			
PH_3	−685.099867	L-1	−684.964151	85.2	3	−685.101377	−0.9
		R-1	−684.964151	85.2	4	−685.105616	−3.6
		I-1	−684.928511	107.5	6	−685.105661	−3.6
		2	−685.084671	9.5			
SiH_3	−581.720792	L-1	−581.619653	63.5	3	−581.724373	−2.2
		R-1	−581.619653	63.5	4	−581.728516	−4.8
		I-1	−581.541509	112.5	6	−581.728744	−5.0
		2	−581.718606	1.4			
OH_2	−152.328151	L-1	−151.958190	232.2	3	−152.332211	−2.5
		R-1	−151.958190	232.2	4	−152.332800	−2.9
		I-1	−152.238018	56.6	6	−152.334543	−4.0
		2	−152.182605	91.3			

[a] VB 8 electrons, except as otherwise noted. All energies are relative to the corresponding *E*(SCFMO) data. [b] VB 12 electrons.

Hartree−Fock. Because VBSCF calculations implicitly include correlation corrections, energies well below Hartree−Fock would be expected, other factors being equal, but all electrons are active in the SCFMO calculations, and only 8 (or 12) electrons are active in the VBSCF calculations. The electrons in the frozen orbitals are unable to adapt to changes in their surroundings, and the resulting adverse effect on energy counterbalances much of the advantage from the inclusion of correlation. In most cases, the 3-structure hybrids **II** afford energies almost as low as the 4- and 6-structure hybrids **III** and **IV**.

In Figure 1a and b, the height of the crossover point depends on the energy difference, *E*, between the reactant at the reactant geometry versus the product geometry and similarly for the product. There is not, however, a simple relation between this height and the barrier to proton transfer (Table 6) for several reasons. One is that the line connecting the reactant at the reactant and product geometries and the analogous line for the product, though shown as straight lines for simplicity, may be curved. Another is that the resonance energy from the mixing of **1** and **2** to give **I** varies from one system to another. Finally, the contribution of **3** and the resonance energy resulting from

TABLE 3: Weights of Resonance Contributors to Transition Structures X−H−X[a]

X	no. of str	weights	X	no. of str	weights
CH_3	2	0.500, 0.500	F	2	0.500, 0.500
	3	0.247, 0.247, 0.506		3	0.204, 0.204, 0.591
	4	0.252, 0.252, 0.476, 0.019		4	0.201, 0.201, 0.576, 0.021
	6	0.270, 0.270, 0.461, −0.007, −0.007, 0.014		6	0.214, 0.214, 0.587, −0.007, −0.007, 0.019
NH_2	2	0.500, 0.500	Cl	2	0.500, 0.500
	3	0.188, 0.188, 0.624		3	0.290, 0.290, 0.420
	4	0.190, 0.190, 0.607, 0.009		4	0.289, 0.289, 0.389, 0.033
	6	0.210, 0.210, 0.587, −0.006, −0.006, 0.006		6	0.292, 0.292, 0.389, −0.002, −0.002, −0.032
PH_2	2	0.500, 0.500	Br	2	0.500, 0.500
	3	0.335, 0.335, 0.331		3	0.333, 0.333, 0.334
	4	0.330, 0.330, 0.303, 0.037		4	0.324, 0.308, 0.308, 0.044
	6	0.330, 0.330, 0.303, −0.000, −0.000, 0.037		6	0.324, 0.324, 0.308, −0.000, −0.000, 0.043
OH	2	0.500, 0.500	NH_3	2	0.500, 0.500
	3	0.187, 0.187, 0.625		3	0.189, 0.189, 0.622
	4	0.147, 0.147, 0.702, 0.003		4	0.193, 0.193, 0.603, 0.010
	6	0.142, 0.142, 0.765, −0.017, −0.017, −0.014		6	0.210, 0.210, 0.584, −0.006, −0.006, 0.007
OH[b]	2	0.500, 0.500	PH_3	2	0.500, 0.500
	3	0.209, 0.209, 0.582		3	0.357, 0.357, 0.286
	4	0.210, 0.210, 0.561, 0.020		4	0.347, 0.347, 0.252, 0.055
	6	0.225, 0.225, 0.549, −0.008, −0.008, 0.016		6	0.343, 0.343, 0.253, 0.002, 0.002, 0.056
SH	2	0.500, 0.500	SiH_3	2	0.500, 0.500
	3	0.206, 0.206, 0.588		3	0.410, 0.410, 0.179
	4	0.195, 0.195, 0.605, 0.004		4	0.391, 0.391, 0.155, 0.062
	6	0.179, 0.179, 0.802, −0.047, −0.047, −0.065		6	0.381, 0.381, 0.158, 0.006, 0.006, 0.069
SH[b]	2	0.500, 0.500	OH_2	2	0.500, 0.500
	3	0.323, 0.323, 0.353		3	0.162, 0.162, 0.676
	4	0.320, 0.320, 0.319, 0.041		4	0.164, 0.164, 0.666, 0.007
	6	0.323, 0.323, 0.319, −0.002, −0.002, 0.039		6	0.179, 0.179, 0.647, −0.006, −0.006, 0.006

[a] VB 8 electrons, except as otherwise noted. [b] VB 12 electrons.

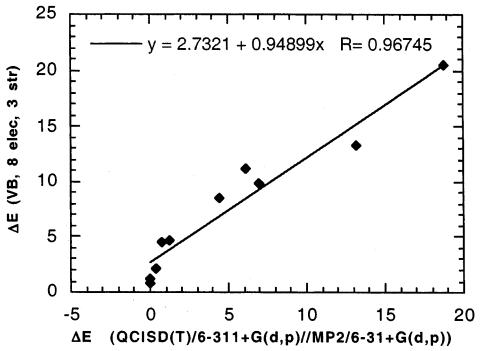

Figure 2. Barrier heights in kilocalories for proton transfer from HX to X^- for 3-structure VB hybrids vs Gaussian values at QCISD(T)/6-311+G(d,p)//MP2/6-31+G(d,p).

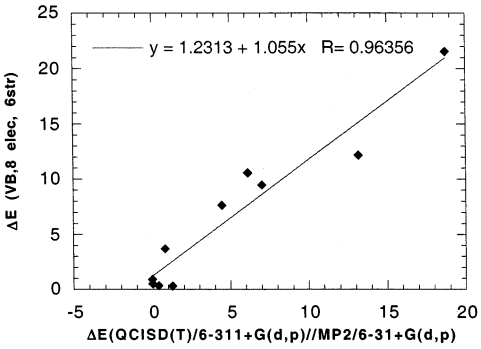

Figure 3. Barrier heights in kcal for proton transfer from HX to X^- for 6-structure VB hybrids vs Gaussian values at QCISD(T)/6-311+G(d,p)//MP2/6-31+G(d,p).

its inclusion are strongly dependent on the ionic character of the X−H bonds.

The systems with X = CH_3^- and SiH_3^- have large *E* values, and structure **3** is well above 2-structure hybrid **I** in energy. Both of these systems consequently show large barriers to proton transfer. The systems with X = F^- and OH_2 have even larger *E* values, but the energy of structure **3** is substantially below that of two-structure hybrid **I**, resulting in the complete absence of barriers. Compare this case to that of X = Cl^- and Br^-, where *E* is much smaller but the energy of **3** is well above that of two-structure hybrid **I**. In this case, the barriers are so low as to be negligible once the zero-point energy is allowed for, but they are low primarily because of the low *E* rather than the low energy of **3** in the case of X = F^- and OH_2. The virtual flattening of the barrier for X = Cl^- and Br^- is further evident from the fact that the respective complexes have nearly the same ionic character as the transition structures.

Hybrids of at least three contributing structures (**1**−**3**) to give **II** are needed to give reasonable barriers. The inclusion of **4**−**6** to give **III** and **IV** results in smaller further changes in the barriers. Table 7 shows barriers calculated by three high-level ab initio methods with electron correlation. Figures 2 and 3 show plots of the VBSCF barriers against one of these sets, that at QCISD(T)/6-311+G(d,p)//MP2/6-31+G(d,p). The correlations are good for both the 3- and 6-structure hybrids, with the former having a slight advantage in the correlation coefficient. The slopes of both plots are close to unity, but the intercepts indicate a tendency for the VBSCF calculations to overestimate the barriers by 1−3 kcal. Barriers for the second-row hydrides run consistently higher than barriers for the corresponding first-row hydrides in both the VBSCF and SCFMO calculations.

Weights of the contributing structures (Tables 3 and 5) afford insights into structures and electron distributions. In nearly all cases, the transition structure possesses greater ionic character (more positive proton in transit, as shown by the weight of **3**) than the ion−dipole complex. The exceptions are for X = OH, Cl, and Br, where the complex is almost as ionic as the transition structure. Weights of **3** are nearly always lower for the second-row than for the first-row transition structures. An important

TABLE 4: Energies of Resonance Contributors and Hybrids for Reactant Complexes XH-- -X[a]

X	*E*(HF/6-31G)	structures	*E*(str)	*E*(rel)	structures	*E*(str)	*E*(rel)
CH_3	−79.641960	L-1	−79.614132	17.5	3	−79.651085	−5.7
		R-1	−79.287249	222.6	4	−79.651229	−5.8
		I-1	−79.479403	102.0	6	−79.651630	−6.1
		2	−79.620090	13.7			
NH_2	−111.647968	L-1	−111.554792	58.5	3	−111.656171	−5.1
		R-1	−111.328198	200.7	4	−111.656400	−5.3
		I-1	−111.587273	38.1	6	−111.656687	−5.5
		2	−111.529931	74.1			
PH_2	−684.170665	L-1	−684.150829	12.4	3	−684.182139	−7.2
		R-1	−683.844598	204.6	4	−684.182297	−7.3
		I-1	−683.992457	111.8	6	−684.184069	−8.4
		2	−684.160523	6.4			
OH	−151.356615	L-1	−151.130683	141.8	3	−151.359884	−2.1
		R-1	−151.229896	79.5	4	−151.361179	−2.9
		I-1	−151.351303	3.3	6	−151.363483	−4.3
		2	−151.230778	79.0			
OH[b]	−151.356615	L-1	−151.055027	189.2	3	−151.360789	−2.6
		R-1	−151.165702	119.8	4	−151.362086	−3.4
		I-1	−151.243316	71.1	6	−151.363297	−4.2
		2	−151.246242	69.3			
SH	−796.725550	L-1	−796.683934	26.1	3	−796.730130	−2.9
		R-1	−796.444542	176.3	4	−796.731454	−3.7
		I-1	−796.723461	1.3	6	−796.732509	−4.4
		2	−796.684288	25.9			
SH[b]	−796.725550	L-1	−796.459108	167.2	3	−796.735608	−6.3
		R-1	−796.679452	28.9	4	−796.736334	−6.8
		I-1	−796.550660	109.7	6	−796.737793	−7.7
		2	−796.704088	13.5			
F	only sym FHF^-						
Cl	−919.600797	L-1	−919.484766	72.8	3	−919.606077	−3.3
		R-1	−919.383935	136.1	4	−919.608470	−4.8
		I-1	−919.447788	96.0	6	−919.608719	−5.0
		2	−919.556748	27.6			
Br	−5140.190573	L-1	−5140.091526	62.2	3	−5140.186605	2.5
		R-1	−5140.002032	118.3	4	−5140.189577	0.6
		I-1	−5140.012425	111.8	6	−5140.189912	0.4
		2	−5140.155691	21.9			
NH_3	−112.727691	L-1	−112.611753	72.8	3	−112.736778	−5.7
		R-1	−112.408436	200.3	4	−112.737164	−5.9
		I-1	−112.605394	76.7	6	−112.737580	−6.2
		2	−112.656832	44.5			
PH_3	−685.109434	L-1	−685.087312	13.9	3	−685.119252	−6.2
		R-1	−684.767717	214.4	4	−685.119496	−6.3
		I-1	−684.911238	124.4	6	−685.122512	−8.2
		2	−685.097429	7.5			
SiH_3	−581.749954	L-1	−581.750794	−0.5	3	−581.756945	−4.4
		R-1	−581.401674	218.5	4	−581.756955	−4.4
		I-1	−581.511725	149.5	6	−581.763078	−8.2
		2	−581.751346	−0.9			
OH_2	only sym (H_2OHOH_2)						

[a] VB 8 electrons, except as otherwise noted. All energies are relative to the corresponding *E*(SCFMO) data. [b] VB 12 electrons.

factor that determines the weight of **3** is the electrostatic stabilization due to the interaction of the central proton with the terminal X groups, either by ion−dipole/induced dipole interactions (in the case of neutral X groups) or by Coulomb interactions (for anionic X groups). The larger radii of second row Xs diminish these interactions and reduce the contribution of **3** to the respective transition states.

Even though the inclusion of the "reversed polarity" structures **4** and **5** lowers the energies of the hybrids somewhat, the weights are either negative or small (<0.01) positive. The SCFMO calculations predict for the case of $X = SiH_3^-$ that the proton in the reactant possesses an excess of negative charge and that a slight excess is still maintained in the transition structure for the proton in transit. In the VBSCF calculations, this would imply that the combined weights of **4**, **5**, and **6** exceed the weight of **3**, which is not the case. The difference may arise from the different basis sets or from the freezing of some electrons in the VBSCF treatment. The weight of the long-bond structure, **6**, is small in most cases but generally somewhat larger for the second-row than for the first-row systems, as might be expected from the greater bonding radii of the heavy atoms in the former.

In summary, VBSCF calculations describe the qualitative characteristics of the complexes and transition structures for proton transfer processes as well as do SCFMO calculations with correlation. They also give a quantitatively respectable account of barrier heights. In addition, the VBSCF calculations provide satisfying analyses of the factors contributing to barrier height. Whereas high-level SCFMO calculations give somewhat better quantitative values for barrier height, they do not offer clear explanations of why barrier heights differ from one system to another.

TABLE 5: Weights of Resonance Contributors to Complexes XH−X[a]

X	no. of str	weights	X	no. of str	weights
CH_3	2	0.977, 0.023	SH[b]	2	0.887, 0.113
	3	0.667, 0.009, 0.324		3	0.626, 0.058, 0.316
	4	0.668, 0.008, 0.322, 0.002		4	0.621, 0.057, 0.311, 0.011
	6	0.660, 0.009, 0.308, 0.021, −0.000, 0.003		6	0.609, 0.058, 0.287, 0.031, −0.001, 0.015
NH_2	2	0.887, 0.113	F		no unsymmetric complex
	3	0.465, 0.036, 0.499	Cl	2	0.701, 0.299
	4	0.467, 0.035, 0.494, 0.004		3	0.432, 0.162, 0.407
	6	0.473, 0.036, 0.495, −0.007, −0.000, 0.003		4	0.429, 0.160, 0.384, 0.026
PH_2	2	0.950, 0.050		6	0.428, 0.164, 0.380, 0.004, −0.002, 0.027
	3	0.690, 0.026, 0.284	Br	2	0.694, 0.306
	4	0.688, 0.025, 0.283, 0.004		3	0.481, 0.189, 0.330
	6	0.668, 0.025, 0.257, 0.044, −0.000, 0.006		4	0.470, 0.185, 0.310, 0.035
OH	2	0.949, 0.051		6	0.464, 0.186, 0.307, 0.009, −0.002, 0.036
	3	0.351, 0.035, 0.614	NH_3	2	0853, 0.147
	4	0.368, 0.041, 0.579, 0.012		3	0.434, 0.046, 0.520
	6	0.308, 0.003, 0.737, 0.001, −0.050, 0.001		4	0.437, 0.045, 0.512, 0.006
OH[b]	2	0.753, 0.247		6	0.445, 0.048, 0.511, −0.007, −0.000, 0.004
	3	0.357, 0.095, 0.548	PH_3	2	0.951, 0.049
	4	0.358, 0.093, 0.534, 0.014		3	0.710, 0.025, 0.266
	6	0.369, 0.101, 0.530, −0.009, −0.003, 0.012		4	0.708, 0.024, 0.264, 0.004
SH	2	0.969, 0.031		6	0.677, 0.025, 0.229, 0.061, −0.000, 0.008
	3	0.509, 0.019, 0.472	SiH_3	2	0.997, 0.003
	4	0.523, 0.019, 0.446, −0.012		3	0.853, 0.001, 0.146
	6	0.376, 0.005, 0.715, 0.000, −0.100, 0.004		4	0.853, 0.001, 0.146, 0.000
				6	0.758, 0.002, 0.111, 0.129, 0.000, 0.001
			OH_2		no unsymmetric complex

[a] VB 8 electrons, except as otherwise noted. [b] VB 12 electrons.

TABLE 6: X−H−X Barriers[a]

X	no. of str	*E*(TS)	*E*(comp)	barrier, kcal	X	no. of str	*E*(TS)	*E*(comp)	barrier, kcal
CH_3	2	−79.593477	−79.62009	16.7	SH[b]	2	−796.698261	−796.704088	3.66
	3	−79.629991	−79.651085	13.24		3	−796.725767	−796.735608	6.18
	4	−79.631157	−79.651229	12.6		4	−796.729019	−796.736334	4.59
	6	−79.632218	−79.65163	12.18		6	−796.729061	−796.737793	5.48
NH_2	2	−111.567211	−111.529931	−23.39	Cl	2	−919.555757	−919.556748	0.62
	3	−111.642512	−111.656171	8.57		3	−919.604118	−919.606077	1.23
	4	−111.643107	−111.6564	8.34		4	−919.607188	−919.60847	0.8
	6	−111.644499	−111.656687	7.65		6	−919.607294	−919.608719	0.89
PH_2	2	−684.147083	−684.160523	8.43	Br	2	−5140.155682	−5140.155691	0.01
	3	−684.166503	−684.182139	9.81		3	−5140.185287	−5140.186605	0.83
	4	−684.168984	−684.182297	8.35		4	−5140.189107	−5140.189577	0.29
	6	−684.168984	−684.184069	9.47		6	−5140.189108	−5140.189912	0.5
OH	2	−151.226214	−151.230778	2.86	NH_3	2	−112.644362	−112.656832	7.82
	3	−151.356582	−151.359884	2.07		3	−112.72956	−112.736778	4.53
	4	−151.359595	−151.361179	0.99		4	−112.730354	−112.737164	4.27
	6	−151.36295	−151.363483	0.33		6	−112.731665	−112.73758	3.71
OH[b]	2	−151.2425	−151.246242	2.35	PH_3	2	−685.084671	−685.097429	8.01
	3	−151.358514	−151.360789	1.43		3	−685.101377	−685.119252	11.22
	4	−151.360302	−151.362086	1.12		4	−685.105616	−685.119496	8.71
	6	−151.362301	−151.363297	0.62		6	−685.105661	−685.122512	10.57
SH	2	−796.680148	−796.684288	2.6	SiH_3	2	−581.718606	−581.751346	20.54
	3	−796.722661	−796.73013	4.69		3	−581.724373	−581.756945	20.44
	4	−796.725275	−796.731454	3.88		4	−581.728516	−581.756955	17.85
	6	−796.732047	−796.732509	0.29		6	−581.728744	−581.763078	21.54

[a] VB 8-electron calculations at HF/6-31G, except as otherwise noted. [b] VB 12-electron calculations.

TABLE 7: XHX Barriers Relative to the Ion−Dipole Complexes at QCISD(T)/6-311+G(d,p)//MP2/6-31+G(d,p), QCISD/6-311+G(d,p)//QCISD/6-311+G(d,p), and QCISD(T)/6-311+G(d,p)//QCISD/6-311+G(d,p)

X	QCISD(T)/MP2 (kcal)	QCISD/QCISD (kcal)	QCISD(T)/QCISD (kcal)
CH_3	13.20[a]	14.62	13.31
NH_2	4.46[a]	6.90	6.29
OH	0.38[a]	0.52	0.4
SiH_3	18.73[a]	17.82	16.28
PH_2	7.02[a]	5.37	4.14
SH	1.27[a]	2.28	1.5
Cl	−0.03[a]	0.00[b]	−0.01[d]
Br	0.00	0.01[c]	−0.04[d]
NH_3	0.80	1.27	0.95
PH_3	6.13	6.99	6.05

[a] From Gronert, S. *J. Am. Chem. Soc.* **1993**, *115*, 10258−10266. [b] Actual value is 0.00044. [c] Actual value is 0.00671. [d] Although the energy of the symmetric XHX is slightly below that of the complex, one negative eigenvalue in the frequency calculation indicates a small barrier.

Supporting Information Available: Tables of energies and weights of contributing structures for simple VB and BOVB calculations made with four active electrons and 6-31G basis sets. This material is available free of charge via the Internet at http://pubs.acs.org.

References and Notes

(1) Gronert, S. *J. Am. Chem. Soc.* **1993**, *115*, 10258−10266.

(2) Stanton, R. V.; Merz, K. M., Jr. *J. Chem. Phys.* **1994**, *101*, 6658−6665.

(3) Harris, N.; Wu, W.; Saunders, W. H., Jr.; Shaik, S. *J. Am. Chem. Soc.* **2000**, *122*, 6754−6758.

(4) Shaik, S. *J. Am. Chem. Soc.* **1981**, *101*, 3692−3701.

(5) Frisch, M. J.; Trucks, G. W.; Schlegel, H. B.; Scuseria, G. E.; Robb, M. A.; Cheeseman, J. R.; Zakrzewski, V. G.; Montgomery, J. A., Jr.; Stratmann, R. E.; Burant, J. C.; Dapprich, S.; Millam, J. M.; Daniels, A. D.; Kudin, K. N.; Strain, M. C.; Farkas, O.; Tomasi, J.; Barone, V.; Cossi, M.; Cammi, R.; Mennucci, B.; Pomelli, C.; Adamo, C.; Clifford, S.; Ochterski, J.; Petersson, G. A.; Ayala, P. Y.; Cui, Q.; Morokuma, K.; Malick,

D. K.; Rabuck, A. D.; Raghavachari, K.; Foresman, J. B.; Cioslowski, J.; Ortiz, J. V.; Stefanov, B. B.; Liu, G.; Liashenko, A.; Piskorz, P.; Komaromi, I.; Gomperts, R.; Martin, R. L.; Fox, D. J.; Keith, T.; Al-Laham, M. A.; Peng, C. Y.; Nanayakkara, A.; Gonzalez, C.; Challacombe, M.; Gill, P. M. W.; Johnson, B. G.; Chen, W.; Wong, M. W.; Andres, J. L.; Head-Gordon, M.; Replogle, E. S.; Pople, J. A. *Gaussian 98*, revision A.6; Gaussian, Inc.: Pittsburgh, PA, 1998.

(6) (a) Wu, W.; Wu, A.; Mo, M.; Lin, M.; Zhang, Q. *Int. J. Quantum Chem.* **1998**, *67*, 287. (b) Wu, W.; Song, L.; Mo, Y.; Zhang, Q. XIAMEN—An Ab Initio Spin-Free Valence Bond Program; Xiamen University: Xiamen, People's Republic of China.

(7) (a) Shurki, A.; Hiberty, P. C.; Shaik, S. *J. Am. Chem. Soc.* **1999**, *121*, 822−834. (b) Hiberty, P. C.; Flament, J. P.; Noizet, E. *Chem. Phys. Lett.* **1992**, *189*, 259.